

Microscopic Origin of Black Hole Reentrant Phase Transitions

M. Kord Zangeneh,^{1,2,*} A. Dehyadegari,^{3,†} A. Sheykhi,^{2,3,‡} and R. B. Mann^{4,§}

¹*Physics Department, Faculty of Science, Shahid Chamran University of Ahvaz, Ahvaz 61357-43135, Iran*

²*Research Institute for Astronomy and Astrophysics of Maragha (RIAAM)-Maragha, IRAN, P. O. Box: 55134-441*

³*Physics Department and Biruni Observatory, Shiraz University, Shiraz 71454, Iran*

⁴*Department of Physics and Astronomy, University of Waterloo, Waterloo, Ontario, Canada, N2L 3G1*

Understanding the microscopic behavior of the black holes ingredients has been one of the important challenges in black holes physics during the past decades. In order to shed some light on the microscopic structure of black holes, in this paper, we explore a recently observed phenomenon for black holes namely reentrant phase transition, by employing the Ruppeiner geometry. Interestingly enough, we observe two properties for the phase behaviour of small black holes that leads to reentrant phase transition. They are correlated and they are of the interaction type. For the range of pressure in which the system underlies reentrant phase transition, it transits from large black holes phase to small one which possesses higher correlation than the other ranges of pressures. On the other hand, the type of interaction between small black holes near large/small transition line, differs for usual and reentrant phase transitions. Indeed, for usual case, the dominant interaction is repulsive whereas for reentrant case we encounter with an attractive interaction. We show that in reentrant phase transition case, the small black holes behave like a Bosonic gas whereas in the usual phase transition case, they behave like a quantum anyon gas.

PACS numbers:

I. INTRODUCTION

A reentrant phase transition (RPT) occurs when a monotonic variation of any thermodynamic quantity gives rise to more than one phase transitions (PTs) such that the initial and final states are macroscopically the same. This phenomenon was first discovered in the nicotine/water mixture during a procedure in which, by increasing the temperature at a sufficient fixed percentage of nicotine, the homogeneous mixed state separated into distinct nicotine/water phases and then the homogeneous state reappeared [1]. More often, as a result of two (or more) competing driving mechanisms, such behavior has also been observed in multicomponent fluid systems, gels, ferroelectrics, liquid crystals, and binary gases as well as non-commutative spacetimes [2] (for more details, see the review [3]).

In the context of black hole (BH) physics, RPT has been first discovered for four-dimensional Born-Infeld (BI) charged anti-de Sitter (AdS) BHs [4]. In this case, for a certain range of pressures, when temperature is lowered monotonically, a large/small/large BHs reentrant phase transition occurred. Further studies show that for higher than four-dimensional BI-AdS BHs, there is no RPT [5]. In [6], d -dimensional singly-spinning Kerr-AdS BHs were studied and it was shown that RPT appears for $d \geq 6$. Remarkably, in these two BH systems, an RPT is accompanied by Hawking-Page (HP) phase transition. This fact is interesting and important since it has

been shown that the HP phase transition is related to a confinement/deconfinement PT in quark-gluon plasma [7]. More studies on RPT in higher-dimensional single- and multi-spinning Kerr-AdS and Kerr-dS BHs have been carried out in [8–11]. It is worth mentioning that these examples of BH RPTs are accompanied by a jump at the global minimum of the Gibbs free energy. This discontinuity is referred to as zeroth-order PT and seen for instance in superfluidity and superconductivity [12]. Recently, it has been shown that the zeroth-order PT can take place as well in an extended phase space of charged dilaton black holes [13]. RPTs have also been observed in frameworks consisting of higher-curvature corrections [14–18]. In these kinds of gravity theories it is possible to find multiple RPTs, and/or RPTs in which there is no zeroth-order PT, with the RPT taking place by a succession of some first order PTs [14, 16, 17].

In this paper, we explore a possible microscopic origin of the black hole RPT via Ruppeiner geometry [19, 20]. We compare the behaviors of Ricci Scalar of Ruppeiner geometry R (referred to as Ruppeiner invariant) for the situations in which an RPT appears and try to infer its microscopic origin. We do this in the case of BI-AdS BHs as well as singly-spinning Kerr-AdS BHs. The sign of the Ruppeiner invariant indicates the dominant interaction between possible molecules of a BH ($R > 0$: repulsion, $R < 0$: attraction and $R = 0$: no interaction) [21–23], while its magnitude is a measure of the average number Planck areas on the event horizon that are correlated with each other [24] (for more information, see [25, 26] and references therein). We note that the microscopic behavior of possible BH molecules has been previously studied via Ruppeiner geometry [27–30].

Our paper is organized as follows. In section II, we review the subject of RPT in the context of black hole

*Electronic address: kordzangeneh.mehdi@gmail.com

†Electronic address: adehyadegari@shirazu.ac.ir

‡Electronic address: asheykhi@shirazu.ac.ir

§Electronic address: rbmann@uwaterloo.ca

thermodynamics. For this purpose, we shall consider two cases: static AdS black holes in the presence of nonlinear BI electrodynamics and spinning Kerr-AdS black holes. We shall use the terminology SPT (for standard phase transition) to denote any phase transition that is not reentrant (i.e. not RPT), whereas PT shall refer to any possible phase transition without distinction. In section III, we study the Ruppeiner geometry of SPTs and RPTs to understand the microscopic origin of the latter. In section IV, we summarize the results we found in this paper.

II. REVIEW OF BLACK HOLE RPT

In this section, we review thermodynamics of higher-dimensional BI-AdS BHs as well as singly-spinning Kerr-AdS BHs and discuss the situations under which the RPT appears in these configurations. Our discussions here are based on Refs. [5] and [6].

A. BI-AdS black holes

The metric of d -dimensional BI-AdS BH is

$$ds^2 = -f(r)dt^2 + \frac{dr^2}{f(r)} + r^2 d\Omega_{d-2}^2, \quad (1)$$

in which $d\Omega_{d-2}^2$ is the line element of $(d-2)$ -dimensional hypersurface with constant scalar curvature $(d-2)(d-3)$ and volume ω and

$$\begin{aligned} f(r) = & 1 + \frac{r^2}{l^2} - \frac{m}{r^{d-3}} \\ & + \frac{4b^2 r^2}{(d-1)(d-2)} \left(1 - \sqrt{1 + \frac{(d-2)(d-3)q^2}{2b^2 r^{2d-4}}} \right) \\ & + \frac{2(d-2)q^2}{(d-1)r^{2d-4}} \\ & \times {}_2F_1 \left[\frac{d-3}{2d-4}, \frac{1}{2}, \frac{3d-7}{2d-4}, -\frac{(d-2)(d-3)q^2}{2b^2 r^{2d-4}} \right], \end{aligned} \quad (2)$$

where l is the AdS radius of spacetime, m and q are related to total mass and charge of BH as

$$Q = \frac{q\omega}{4\pi} \sqrt{\frac{(d-2)(d-3)}{2}}, \text{ and } M = \frac{(d-2)m\omega}{16\pi}, \quad (3)$$

where ω represents the area of the unit $(d-2)$ -sphere. Using the fact that $f(r_+) = 0$ where r_+ is the radius of outermost horizon, we can find the constant m in terms

of r_+ and express the total mass of BH as function of r_+ ,

$$\begin{aligned} M = & \frac{(d-2)\omega r_+^{d-3}}{16\pi} \left[1 + \frac{r_+^2}{l^2} \right. \\ & + \frac{4b^2 r_+^2}{(d-1)(d-2)} \left(1 - \sqrt{1 + \frac{16\pi^2 Q^2}{b^2 \omega^2 r_+^{2d-4}}} \right) \\ & + \frac{64\pi^2 Q^2}{(d-1)(d-3)\omega^2 r_+^{2d-6}} \\ & \left. \times {}_2F_1 \left[\frac{d-3}{2d-4}, \frac{1}{2}, \frac{3d-7}{2d-4}, -\frac{16\pi^2 Q^2}{b^2 \omega^2 r_+^{2d-4}} \right] \right]. \end{aligned} \quad (4)$$

In the above expression b is the nonlinear BI parameter appears in the BI Lagrangian, $L_{BI} = 4b^2(1 - \sqrt{1 + F^{\mu\nu}F_{\mu\nu}/2b^2})$. The electrodynamics field tensor $F_{\mu\nu} = \partial_{[\mu}A_{\nu]}$ and gauge potential $A_\nu = (A_t, 0, 0, \dots)$ is given by

$$\begin{aligned} A_t = & -\frac{q}{r^{d-3}} \sqrt{\frac{d-2}{2(d-3)}} \\ & \times {}_2F_1 \left[\frac{d-3}{2d-4}, \frac{1}{2}, \frac{3d-7}{2d-4}, -\frac{(d-2)(d-3)q^2}{2b^2 r^{2d-4}} \right]. \end{aligned} \quad (5)$$

In the limiting case where $b \rightarrow \infty$, the BI Lagrangian reproduces the linear Maxwell one. The electromagnetic potential defined by

$$\Phi = A_\mu \chi^\mu|_{r \rightarrow \infty} - A_\mu \chi^\mu|_{r=r_+}, \quad (6)$$

where $\chi = \partial_t$ is the Killing vector, can also be calculated as

$$\begin{aligned} \Phi = & \frac{4\pi Q}{(d-3)\omega r_+^{d-3}} \\ & \times {}_2F_1 \left[\frac{d-3}{2d-4}, \frac{1}{2}, \frac{3d-7}{2d-4}, -\frac{16\pi^2 Q^2}{b^2 \omega^2 r_+^{2d-4}} \right]. \end{aligned} \quad (7)$$

The cosmological constant is fixed as $\Lambda = -(d-1)(d-2)/2l^2$ and related to the thermodynamic pressure as (in Planck unit) [31–34]

$$P = -\frac{\Lambda}{8\pi} = \frac{(d-1)(d-2)}{16\pi l^2}. \quad (8)$$

The corresponding Hawking temperature associated with the event horizon r_+ , and the entropy of BH are given by

$$\begin{aligned} T = & \frac{1}{4\pi} \left[\frac{(d-1)r_+}{l^2} + \frac{(d-3)}{r_+} \right. \\ & \left. + \frac{4b^2 r_+}{d-2} \left(1 - \sqrt{1 + \frac{16\pi^2 Q^2}{b^2 \omega^2 r_+^{2d-4}}} \right) \right], \end{aligned} \quad (9)$$

$$S = \frac{\omega r_+^{d-2}}{4}. \quad (10)$$

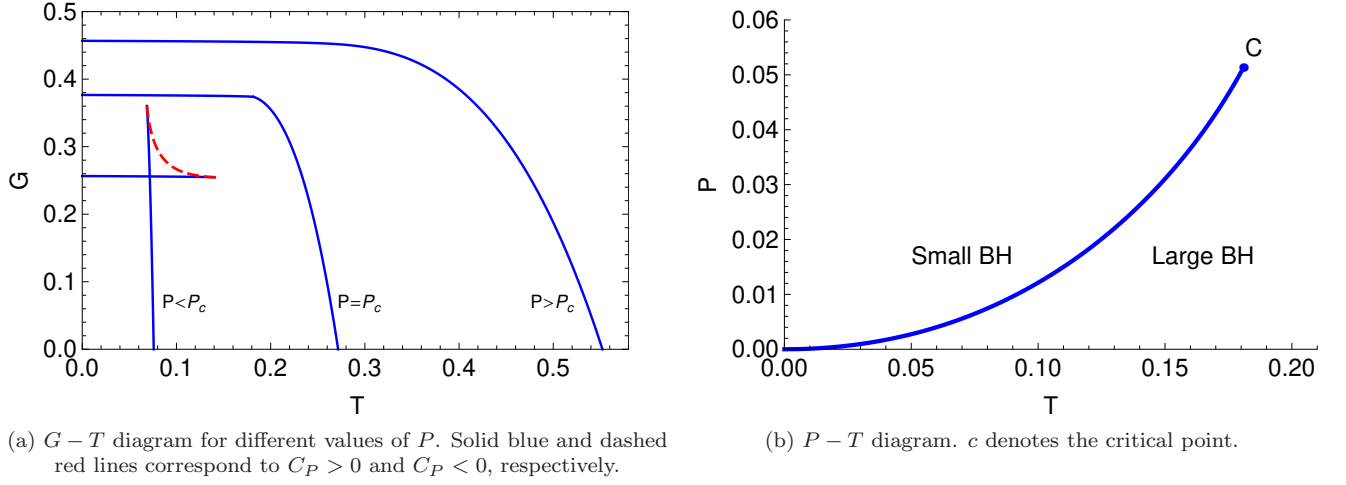


FIG. 1: The behavior of G and P versus T for 5-dimensional BI-AdS BHs with $Q = 1$ and $b = 0.035$ where $(P_c, T_c) = (0.051, 0.181)$. This behavior is the same for $(n \geq 5)$ -dimensional BI-AdS and 4- and 5-dimensional Kerr-AdS BHs.

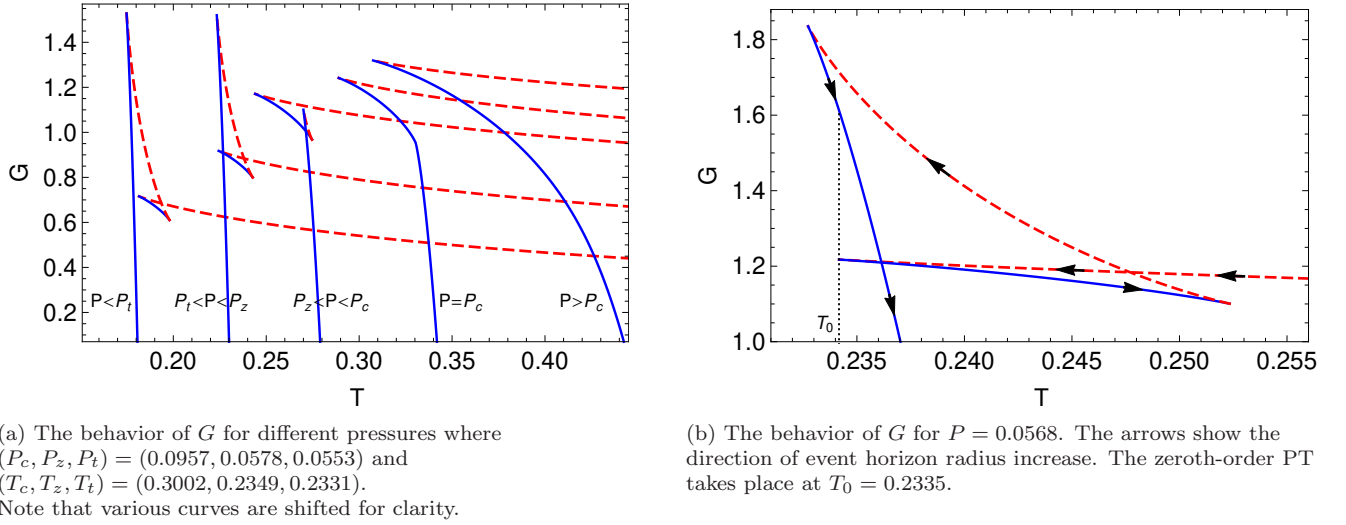


FIG. 2: The behavior of G versus T for 6-dimensional Kerr-AdS black hole with $J = 1$. Solid blue and dashed red lines are corresponding respectively to $C_P > 0$ and $C_P < 0$. This behavior is qualitatively the same for 4-dimensional BI-AdS and $(n \geq 6)$ -dimensional Kerr-AdS BHs.

Interpreting the mass of BH, M , as the enthalpy rather than the internal energy of the gravitational system [32], we can write the first law of thermodynamics as

$$dM = TdS + \Phi dQ + VdP + \mathfrak{B}db, \quad (11)$$

in which M is a function of BI coupling coefficient as well as other usual thermodynamic parameters [35]. The

conjugate quantity of b is given by

$$\begin{aligned} \mathfrak{B} = & \frac{\omega b r_+^{d-1}}{2(d-1)\pi} \left(1 - \sqrt{1 + \frac{16\pi^2 Q^2}{b^2 \omega^2 r_+^{2d-4}}} \right) \\ & + \frac{4Q^2 \pi}{(d-1)b\omega r_+^{d-3}} \\ & \times {}_2F_1 \left[\frac{d-3}{2d-4}, \frac{1}{2}, \frac{3d-7}{2d-4}, -\frac{16\pi^2 Q^2}{b^2 \omega^2 r_+^{2d-4}} \right]. \end{aligned} \quad (12)$$

which is referred to as ‘BI vacuum polarization’. Also, the thermodynamic volume conjugate to the pressure is $V = \omega r_+^{d-1}/(d-1)$. The generalized Smarr formula in the extended phase space can be obtained by scaling ar-

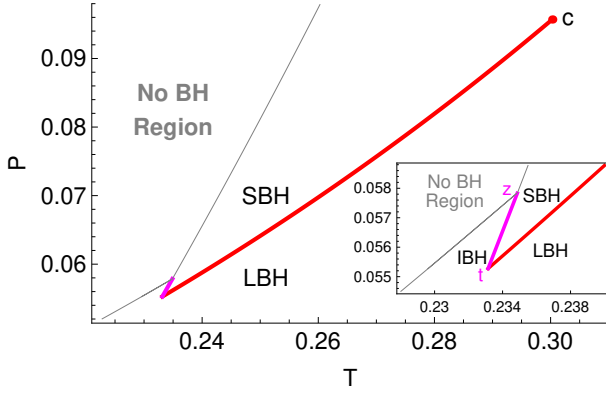


FIG. 3: Phase diagram for 6-dimensional Kerr-AdS BH with $J = 1$. c denotes the critical point. We zoom in on RPT region to make it more clear. NO BH REGION corresponds to a forbidden region of parameter space. This behavior is the same for $(n \geq 6)$ -dimensional Kerr-AdS and 4-dimensional BI-AdS BHs.

gument as

$$M = \frac{d-2}{d-3}TS + \Phi Q - \frac{2}{d-3}VP - \frac{1}{d-3}\mathfrak{B}b. \quad (13)$$

To examine the PT behaviors (or thermodynamic behaviors), in addition to the equation of state $T = T(P, V)$, which can be calculated by eliminating l^2 between (8) and (9), we study the Gibbs free energy $G = M - TS$,

$$\begin{aligned} G(T, P) = & \frac{\omega}{16\pi} \left[r_+^{d-3} - \frac{16\pi P r_+^{d-1}}{(d-1)(d-2)} \right. \\ & - \frac{4b^2 r_+^{d-1}}{(d-1)(d-2)} \left(1 - \sqrt{1 + \frac{16\pi^2 Q^2}{b^2 \omega^2 r_+^{2d-4}}} \right) \\ & + \frac{64(d-2)^2 \pi^2 Q^2}{(d-1)(d-3)\omega^2 r_+^{d-3}} \\ & \left. \times {}_2F_1 \left[\frac{d-3}{2d-4}, \frac{1}{2}, \frac{3d-7}{2d-4}, -\frac{16\pi^2 Q^2}{b^2 \omega^2 r_+^{2d-4}} \right] \right]. \end{aligned} \quad (14)$$

Note that in our study on BI-AdS BH, we treat Q and b as fixed variables.

B. Singly-spinning Kerr-AdS black holes

In d -dimensional spacetime the metric of singly spinning Kerr-AdS black holes may be written

$$\begin{aligned} ds^2 = & -\frac{\Delta}{\rho^2} \left(dt - \frac{a}{\Xi} \sin^2 \theta d\varphi \right)^2 + \frac{\rho^2}{\Delta} dr^2 + \frac{\rho^2}{\Sigma} d\theta^2 \\ & + \frac{\Sigma \sin^2 \theta}{\rho^2} \left[a dt - \frac{(r^2 + a^2)}{\Xi} d\varphi \right]^2 + r^2 \cos^2 \theta d\Omega_{d-2}^2, \end{aligned} \quad (15)$$

where

$$\begin{aligned} \Delta &= (r^2 + a^2) \left(1 + \frac{r^2}{l^2} \right) - \frac{2m}{r^{d-5}}, \quad \Xi = 1 - \frac{a^2}{l^2}, \\ \Sigma &= 1 - \frac{a^2}{l^2} \cos^2 \theta \quad \text{and} \quad \rho^2 = r^2 + a^2 \cos^2 \theta. \end{aligned} \quad (16)$$

The associated thermodynamic quantities read (in Planck units)

$$M = \frac{\omega}{4\pi} \frac{m}{\Xi^2} \left(1 + \frac{(d-4)\Xi}{2} \right), \quad (17)$$

$$J = \frac{\omega}{4\pi} \frac{ma}{\Xi^2}, \quad (18)$$

$$\Omega_H = \frac{a}{l^2} \frac{r_+^2 + l^2}{r_+^2 + a^2}, \quad (19)$$

$$P = \frac{-\Lambda}{8\pi} = \frac{(d-1)(d-2)}{16\pi l^2}, \quad (20)$$

$$T = \frac{1}{2\pi} \left[\left(1 + \frac{r_+^2}{l^2} \right) \left(\frac{r_+}{a^2 + r_+^2} + \frac{d-3}{2r_+} \right) - \frac{1}{r_+} \right], \quad (21)$$

$$S = \frac{\omega}{4} \frac{(a^2 + r_+^2) r_+^{d-4}}{\Xi}, \quad (22)$$

where m can be calculated by setting $\Delta(r_+) = 0$. We find

$$m = (r_+^2 + a^2) \left(\frac{r_+^{d-5}}{2} + \frac{r_+^{d-3}}{2l^2} \right). \quad (23)$$

One can also find the first law of BH thermodynamics and Smarr formula as [32]

$$dM = TdS + \Omega_H dJ + VdP, \quad (24)$$

$$\frac{d-3}{d-2}M = TS + \Omega_H J - \frac{2}{d-2}VP, \quad (25)$$

where the volume conjugate to pressure is

$$V = \frac{\omega r_+^{d-1}}{d-1} \left[1 + \frac{a^2}{\Xi} \frac{1 + r_+^2/l^2}{(d-2)r_+^2} \right]. \quad (26)$$

The Gibbs free energy $G = M - TS$ governing the thermodynamic behavior of the system reads

$$\begin{aligned} G(T, P, J) = & \frac{\omega r_+^{d-5}}{16\pi \Xi^2} \\ & \times \left(3a^2 + r_+^2 - \frac{(r_+^2 - a^2)^2}{l^2} + \frac{3a^2 r_+^4 + a^4 r_+^2}{l^4} \right). \end{aligned} \quad (27)$$

Eliminating m , a and r_+ in Eqs. (17)-(22) in terms of the basic thermodynamic variables, one can numerically obtain the equation of state $T = T(P, V)$ in the canonical ensemble (with fixed J).

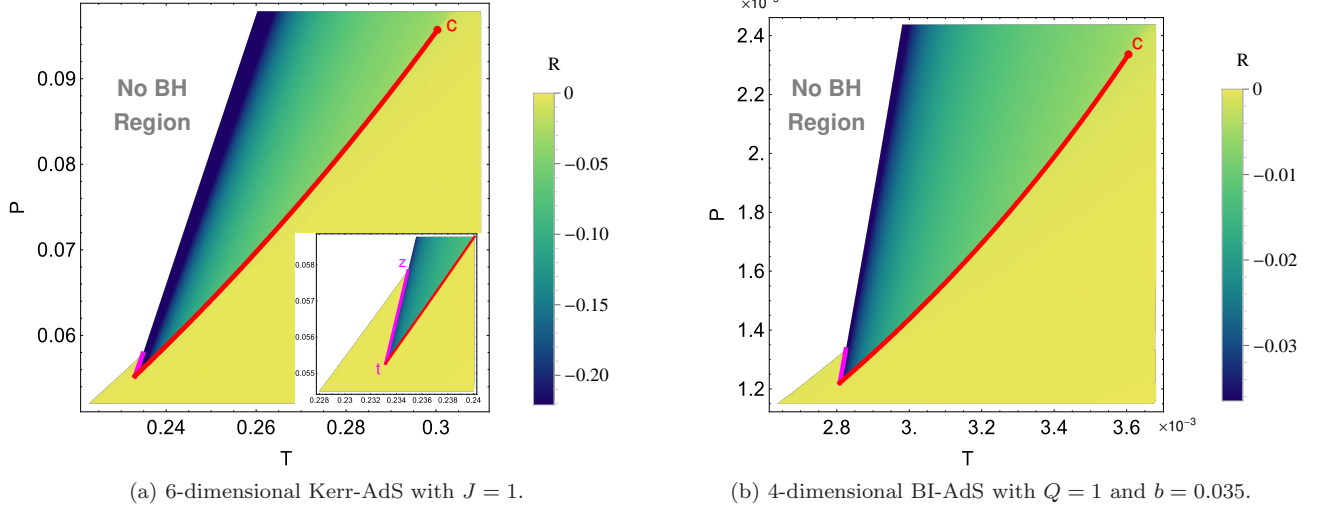


FIG. 4: The $R - P - T$ diagram for 4-dimensional BI-AdS and 6-dimensional Kerr-AdS BHs. This behavior is the same for $(n \geq 6)$ -dimensional Kerr-AdS and 4-dimensional BI-AdS BHs.

C. Reentrant phase transition

The thermal stability of a thermodynamic system may be determined by the sign of system's response functions. One of these response functions is specific heat at constant pressure. For the BHs under consideration, the specific heat is given by

$$C_P = T \left(\frac{\partial S}{\partial T} \right)_{P, \{Y\}} \quad \{Y\} = \begin{cases} b, Q & \text{for BI-AdS} \\ J & \text{for Kerr-AdS} \end{cases} \quad (28)$$

Positivity (negativity) of C_P determines the local stability (instability) which is shown by solid blue (dashed red) lines in a $G - T$ diagram (see Figs. 1(a) and 2). In order to examine the precise behavior of the system, we investigate the behavior of the Gibbs free energy G . For 5-dimensional BI-AdS black holes this is plotted in Fig. 1(a). From this figure, we see that for $P > P_c$, G has smooth behavior as a function of T , whereas for $P < P_c$ it exhibits multi-valued behavior related to the LBH/SBH (large black hole/small black hole) first order SPT that is similar to the SPT of the Van der Waals fluid system. The corresponding phase diagram is shown in Fig. 1(b) in which for $P < P_c$ and $T < T_c$, large and small BH phases are separated by the transition line. This kind of behavior is observed for $(d \geq 5)$ -dimensional BI-AdS BHs and also 4- and 5-dimensional Kerr-AdS BHs.

However for 4-dimensional BI-AdS BHs and $(d \geq 6)$ -dimensional Kerr-AdS BHs, the thermodynamic behaviour is different. The behaviour of the Gibbs free energy for 6-dimensional Kerr-AdS BHs versus temperature for fixed pressure is plotted in Fig. 2(a). As one can see, for $P > P_c$ the behavior of the system is similar to that of Schwarzschild-AdS BHs: the upper (lower) branch corresponds to small (large) BHs with $C_P < 0$ ($C_P > 0$) and at $G(T_{HP}, P_{HP}) = 0$, the Hawking-Page

SPT occurs. Decreasing the pressure to $P = P_c$, we have an additional second order PT at $T = T_c$ in comparison with $P > P_c$ case. In the region $P_t < P < P_c$, a LBH/SBH first order SPT takes place which is similar to liquid/gas Van der Waals SPT (note that P_t shows the end of a transition line corresponding to the first order SPT). In the region $P_t < P < P_z$, according to the behavior of Gibbs free energy, we have a zeroth-order PT besides the LBH/SBH first order PT (see Fig. 2(b)). Note that P_z determines the starting point for observing zeroth-order PT. This kind of phase transition takes place by a discontinuity in Gibbs free energy that gives rise to a small/large (intermediate) BHs PT. Therefore, generally we have a LBH/SBH/LBH phase transition – this is an RPT since the starting and ending phases are macroscopically similar. For $P < P_t$ the situation is the same as $P > P_c$ case; note that since the black hole has charge a Hawking-Page PT (which would not conserve charge) does not take place.

The phase diagram corresponding to an RPT is depicted in the $P - T$ diagram in Fig. 3. The solid lines are coexistence lines denoting the boundary of two different phases. The inset shows that for $P > P_z$ there is a SPT, whereas for $P < P_t$ there is no PT, even where G changes sign. The RPT occurs for $P_t < P < P_z$, where the red line signifies a first-order PT and the magenta line signifies a zeroth-order PT. Note that there is a forbidden region in parameter space for which no black hole solutions exist. Similar RPT behavior takes place for 4-dimensional BI-AdS as well as $(d \geq 6)$ -dimensional Kerr-AdS BHs [4, 6].

For $P_t < P = 0.0567 < P_z$ an RPT corresponding to a 6-dimensional Kerr-AdS BHs is depicted in Fig. 2(b). The direction of arrows follows increasing horizon radius. As temperature decreases the system always moves on the lower branch in each region to maintain thermo-

dynamic equilibrium. Beginning on the lower steeply-sloped curve, a first order PT takes place after which the system is on the near-flat blue curve. This is an SPT from an LBH to an SBH. At $T = T_0$, a zeroth-order PT takes place at which a finite jump in G takes place and the system moves back to the steep blue curve. This finite jump is a zeroth-order PT between an SBH and an IBH (an LBH but of smaller radius). The entire process is an RPT.

III. MICROSCOPIC ORIGIN OF THE BLACK HOLE RPT

In this section, we will study the microscopic origin of black holes RPT by adopting the Ruppeiner approach towards thermodynamic geometry of BHs [21–26]. We define the Ruppeiner metric in $X^\alpha = (M, Z)$ space where $Z = Q$ for BI-AdS BHs and $Z = P$ for Kerr-AdS BHs. The entropy S leads to the thermodynamic potential,

$$g_{\alpha\beta} = -\frac{\partial^2 S}{\partial X^\alpha \partial X^\beta}. \quad (29)$$

The above metric can also be rewritten in the Weinhold form

$$g_{\alpha\beta} = \frac{1}{T} \frac{\partial^2 M}{\partial Y^\alpha \partial Y^\beta}, \quad (30)$$

where $Y^\alpha = (S, Z)$. The Ricci scalar corresponding to this metric is referred to as Ruppeiner invariant R , and can give us some information about the microscopic behavior of possible BH molecules. The sign of R signifies the dominant interaction between microscopic constituents of a system (the possible BH molecules in our case): positive, negative and zero values respectively indicate repulsion, attraction, and no interaction [21–23]. Its magnitude provides a measure of the average number of correlated constituents [24]; for black holes this would be the average number of correlated Planck areas on the event horizon.

In order to study the microscopic origin of an RPT, we examine the behavior of the Ruppeiner invariant on both sides of the coexistence lines in the $P - T$ diagram. We illustrate this in Fig. 4 for both 4-dimensional BI-AdS black holes and for 6-dimensional singly spinning Kerr-AdS blackholes; note that both diagrams are similar to 3. Since there are two PT in case of RPT, we have two transition lines. The rightmost and leftmost transition lines are respectively related to LBH/SBH and SBH/IBH (a smaller LBH) PTs as temperature is decreased.

We see for both cases that $R < 0$, indicating that the dominant interaction is attractive. The important point we can understand from Fig. 4 is that for the zeroth-order PT R is much more negative in going from the SBH to the IBH than in going from the LBH to the SBH. For the RPT, R goes from small negative (LBH) to larger negative (SBH) back to small negative (IBH) again by decreasing the temperature at fixed pressure. According

to the definition of RPT, we know that the starting and ending phases should be the same macroscopically. From Fig. 4 we see that, they are almost the same too, from a microscopic point of view, since the magnitude and sign of the Ruppeiner invariant R are the same on these phases.

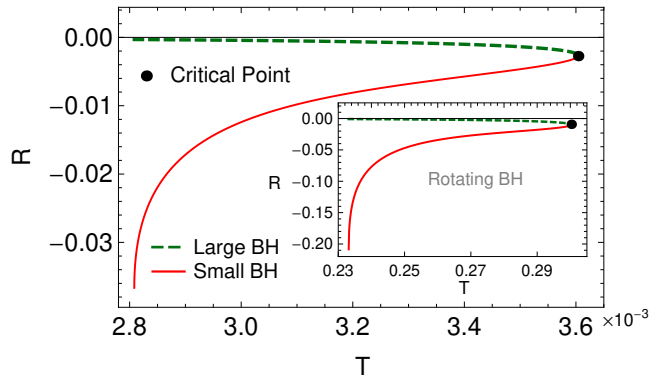


FIG. 5: The behavior of the Ruppeiner invariant R along the rightmost transition line (the red line in Fig. 4) for 4-dimensional BI-AdS and 6-dimensional Kerr-AdS BHs. For $(n \geq 6)$ -dimensional Kerr-AdS BHs, this behavior is qualitatively the same.

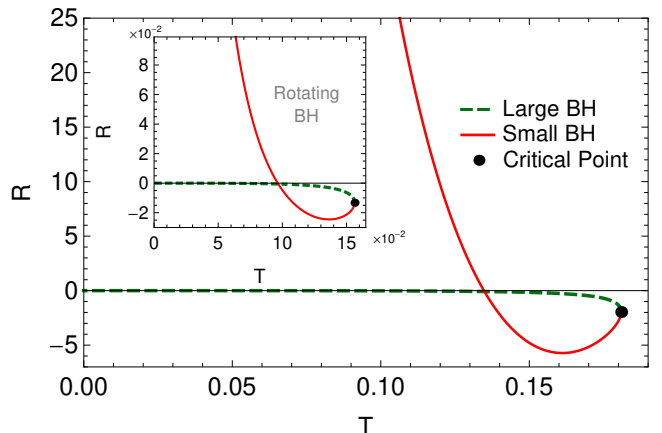


FIG. 6: The behavior of Ruppeiner invariant R along the transition line for 5-dimensional BI-AdS in Fig. 1(b) and Kerr-AdS BHs with $J = 1$, with the values of b and Q as in Fig. 1. For $(n \geq 5)$ -dimensional BI-AdS and 4- and 5-dimensional Kerr-AdS BHs, the behavior is qualitatively the same.

We see from Fig. 4 that when we move downward through the rightmost transition line, the value of R for points close to the line and on its right side (i.e. the LBH phase) is near zero. This behaviour can be seen more clearly in Fig. 5. For the usual first-order PT, the magnitude of the Ruppeiner invariant R for the LBH phase near the transition line is almost the same as for the IBH i.e. it is near zero. For these black holes their microscopic constituents attract and have weak correlation. This behaviour is expected for large BHs where micro-

scopic ingredients of BH are expected to be far from each other.

However, for the SBH phase, the microscopic behaviour of BHs underlying the usual PT and RPTs are different near the transition line. For the underlying RPT, as we move downward near the coexistence line in Fig. 5 on its left side, the Ruppeiner invariant is negative and of increasing magnitude. The dominant interaction is attractive, with the constituents much more strongly correlated.

The behaviour of R for the usual SPT in Fig. 1(b) is illustrated in Fig. 6. In this case, the value R near the coexistence line for the SBH is negative at critical point but passes through zero toward increasingly positive values (signifying increasing correlation for repulsively interacting constituents) as the temperature decreases; the value of R is positive infinite near zero temperature. We know that for SBHs near the transition line, the pressure is low when temperature is low, as is clear from Fig. 1(b). In this region of the phase diagram for the SBH the repulsion is high; despite this, the pressure is low. Evidently the effects of low temperature dominate over this repulsion, ‘freezing’ the black hole molecules and increasing their correlation. The LBH always has weak attraction and low correlation amongst its constituents.

It is worth noting that the RPT occurs in a special region of low pressures $P_t < P < P_z$, shown in Fig. 4. For a given pressure in this region, by decreasing the temperature we transit from an LBH to an SBH of greater $|R|$, indicating greater correlations in comparison to other ranges of pressure. This high correlation becomes higher as we decrease the temperature further in this pressure range. One of the signs of a PT is a change from low to high correlation amongst constituents (or vice-versa). It seems that from a microscopic point of view, the difference making the BH system able to undergo an RPT for this special region of pressure $P_t < P < P_z$ is the greater correlation between molecules of SBHs in comparison to other ranges of pressure.

Here, a question may arise when one compares the behaviour of the Ruppeiner invariant R for BH configurations exhibiting an RPT and ones exhibiting an SPT. For the latter, the correlation (the magnitude of R) is high for small BHs near transition line for low pressures as one can see from Fig. 6 (note from Fig. 1(b) that along transition line low temperatures lead to low pressures). Furthermore, as one can see in Fig. 7, for a given (low) pressure, when the temperature decreases and system transits to an SBH phase, the correlation (the magnitude of R) increases as temperature decreases more in this phase. The SPT/RPT distinction is evidently one of increasing repulsion/attraction for an SBH relative to the LBH. The attraction may help the SBH to undergo an additional zero-order PT as temperature decreases (hence an RPT) whereas the increasing repulsion obstructs an additional phase transitions (hence an SPT).

As one can see in Fig. 7, the BH configuration with SPT shows two different behaviors by decreasing the tem-

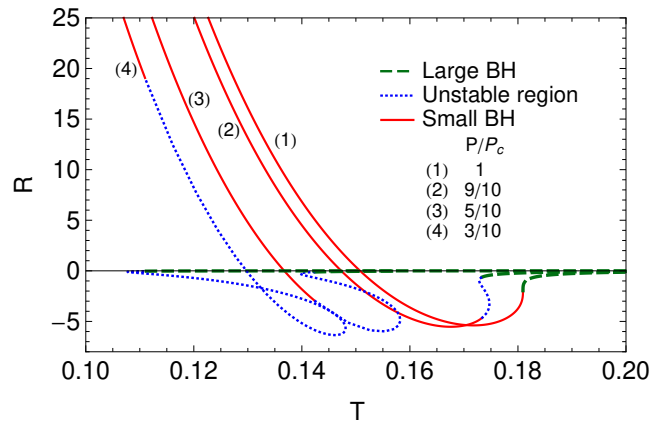


FIG. 7: The behavior of Ruppeiner invariant R for different given pressures for 5-dimensional BI-AdS BH with $Q = 1$ and $b = 0.035$. For other configurations underlying usual PT, the behavior is the same.

perature from high to low values for a given pressure. A part of this behavior for high temperatures carries the Bosonic negative sign whereas another part for low temperatures looks like a Fermionic gas. Similar behavior has been observed for a quantum gas of anyons where the molecular volume is fixed [26]. The blue dotted lines in Fig. 7 correspond to the swallow tail part of the $G-T$ diagram for $P < P_c$ (Fig. 1(a)). In the swallowtail region, the system has a thermodynamic instability on part of the curve, whereas on the other part the specific heat C_P at fixed P (which determines the local instability) is positive.

IV. SUMMARY AND CONCLUSIONS

In this paper, we investigated the microscopic origin of the reentrant phase transition (RPT) in BHs thermodynamics. For this purpose, we employed the Ruppeiner geometry towards thermodynamics geometry of BHs. We showed that the ending and starting phases which are the same macroscopically, are the same microscopically, too. We found out that there are no microscopic difference between the behavior of large BHs near large-small transition line of usual PT and RPT cases, and the main difference is in the microscopic behavior of small black holes. We observed that for usual PT, the dominant interaction for small BHs near transition line for low temperatures is repulsive whereas for RPT it is attractive.

The fact that we have two phase transitions in RPT case, for the pressure in the range of $P_t < P < P_z$, can be understood easily (see Fig. 2(a)). Indeed, in this region the system transits from large BH to small one with higher correlations compared to the other regions of pressure. We showed that with decreasing the temperature of a given pressure P , correlation becomes higher and it makes the system possible to underlie another phase transition in the region $P_t < P < P_z$.

We also explored the microscopic origin of black holes RPT by adopting the Ruppeiner approach towards thermodynamic geometry of BHs. It is well-known that the magnitude of the Ruppeiner invariant R measures the average number of Planck areas on the event horizon correlated to each other or roughly speaking correlation [24]. We examined the behaviour of the Ruppeiner invariant on both sides of transition lines in $P - T$ diagram (see Fig. 4). We observed that in RPT case the small BHs behave like a Bosonic gas whereas in the usual PT case small black holes behave like a quantum anyon gas. We showed that the freezing is more effective than the dominant interaction at low temperature since in both the two kinds of phase transitions (namely the usual PT and

RPT) have low pressure in this region despite different interactions.

Acknowledgments

We are grateful to Prof. Bin Wang for useful discussions and helpful comments. AD and AS thank the research council of Shiraz University. The work of MKZ has been supported financially by Research Institute for Astronomy & Astrophysics of Maragha (RIAAM) under research project No. 1/5237-57.

-
- [1] C. Hudson, *Die gegenseitige Islichkeit von nikotin in wasser*, Z. Phys. Chem. **47** (1904) 113.
 - [2] O. Panella and P. Roy, *Re-entrant phase transitions in non-commutative quantum mechanics*, J. Phys. Conf. Ser. **670** (2016) 012040.
 - [3] T. Narayanan and A. Kumar, *Reentrant phase transitions in multicomponent liquid mixtures*, Physics Reports **249** (1994) 135.
 - [4] S. Gunasekaran, R. B. Mann and D. Kubiznak, *Extended phase space thermodynamics for charged and rotating black holes and Born-Infeld vacuum polarization*, JHEP **1211** (2012) 110 [arXiv:1208.6251].
 - [5] D. C. Zou, S. J. Zhang and B. Wang, *Critical behavior of Born-Infeld AdS black holes in the extended phase space thermodynamics*, Phys. Rev. D **89** (2014) 044002 [arXiv:1311.7299].
 - [6] N. Altamirano, D. Kubiznak and R. B. Mann, *Reentrant phase transitions in rotating anti-de Sitter black holes*, Phys. Rev. D **88** (2013) 101502 [arXiv:1306.5756].
 - [7] E. Witten, *Anti-de Sitter Space, Thermal Phase Transition, And Confinement In Gauge Theories*, Adv. Theor. Math. Phys. **2** (1998) 505 [hep-th/9803131].
 - [8] N. Altamirano, D. Kubiznak, R. B. Mann and Z. Sherkatghanad, *Kerr-AdS analogue of triple point and solid/liquid/gas phase transition*, Class. Quant. Grav. **31** (2014) 042001 [arXiv:1308.2672].
 - [9] N. Altamirano, D. Kubiznak, R. B. Mann and Z. Sherkatghanad, *Thermodynamics of rotating black holes and black rings: phase transitions and thermodynamic volume*, Galaxies **2** (2014) 89 [arXiv:1401.2586].
 - [10] D. Kubiznak and F. Simovic, *Thermodynamics of horizons: de Sitter black holes and reentrant phase transitions*, Class. Quant. Grav. **33** (2016) 245001 [arXiv:1507.08630].
 - [11] S. W. Wei, P. Cheng and Y. X. Liu, *Analytical and exact critical phenomena of d-dimensional singly spinning Kerr-AdS black holes*, Phys. Rev. D **93** (2016) 084015 [arXiv:1510.00085].
 - [12] V. P. Maslov, *Zeroth-order phase transitions*, Mathematical Notes **76** (2004) 697.
 - [13] A. Dehyadegari, A. Sheykhi and A. Montakhab, *Novel phase transition in charged dilaton black holes*, arXiv:1707.05307.
 - [14] A. M. Frassino, D. Kubiznak, R. B. Mann and F. Simovic, *Multiple Reentrant Phase Transitions and Triple Points in Lovelock Thermodynamics*, JHEP **1409** (2014) 080 [arXiv:1406.7015].
 - [15] S. W. Wei and Y. X. Liu, *Triple points and phase diagrams in the extended phase space of charged Gauss-Bonnet black holes in AdS space*, Phys. Rev. D **90** (2014) 044057 [arXiv:1402.2837].
 - [16] R. A. Hennigar, W. G. Brenna and R. B. Mann, *Pv criticality in quasitopological gravity*, JHEP **1507** (2015) 077 [arXiv:1505.05517].
 - [17] Z. Sherkatghanad, B. Mirza, Z. Mirzaeyan and S. A. H. Mansoori, *Critical behaviors and phase transitions of black holes in higher order gravities and extended phase spaces*, arXiv:1412.5028.
 - [18] R. A. Hennigar and R. B. Mann, *Reentrant phase transitions and van der Waals behaviour for hairy black holes*, Entropy **17** (2015) 8056 [arXiv:1509.06798].
 - [19] G. Ruppeiner, *Thermodynamics: A Riemannian geometric model*, Phys. Rev. A **20** (1979) 1608.
 - [20] G. Ruppeiner, *Riemannian geometry in thermodynamic fluctuation theory*, Rev. Mod. Phys. **67** (1995) 605 [Erratum: Rev. Mod. Phys. **68** (1996) 313].
 - [21] G. Ruppeiner, *Thermodynamic curvature measures interactions*, American Journal of Physics **78** (2010) 1170 [arXiv:1007.2160].
 - [22] G. Ruppeiner, *Thermodynamic Curvature From the Critical Point to the Triple Point*, Phys. Rev. E **86** (2012) 021130 [arXiv:1208.3265].
 - [23] H. O. May, P. Mausbach and G. Ruppeiner, *Thermodynamic Curvature for Attractive and Repulsive Intermolecular Forces*, Phys. Rev. E **88** (2013) 032123.
 - [24] G. Ruppeiner, *Thermodynamic curvature and phase transitions in Kerr-Newman black holes*, Phys. Rev. D **78** (2008) 024016 [arXiv:0802.1326].
 - [25] G. Ruppeiner, *Thermodynamic curvature: pure fluids to black holes*, J. Phys.: Conf. Series **410** (2013) 012138 [arXiv:1210.2011].
 - [26] G. Ruppeiner, *Thermodynamic Curvature and Black Holes*, Springer Proc. Phys. **153** (2014) 179 [arXiv:1309.0901].
 - [27] S. W. Wei and Y. X. Liu, *Insight into the Microscopic Structure of an AdS Black Hole from Thermodynamical Phase Transition*, Phys. Rev. Lett. **115** (2015) 111302 [arXiv:1502.00386].

- [28] M. Kord Zangeneh, A. Dehyadegari and A. Sheykhi, *Comment on "Insight into the Microscopic Structure of an AdS Black Hole from a Thermodynamical Phase Transition"*, arXiv:1602.03711.
- [29] A. Dehyadegari, A. Sheykhi and A. Montakhab, *Critical behaviour and microscopic structure of charged AdS black holes via an alternative phase space*, Phys. Lett. B **768** (2017) 235 [arXiv:1607.05333].
- [30] M. Kord Zangeneh, A. Dehyadegari, M. R. Mehdizadeh, B. Wang and A. Sheykhi, *Thermodynamics, phase transitions and Ruppeiner geometry for Einstein-dilaton Lifshitz black holes in the presence of Maxwell and Born-Infeld electrodynamics*, Eur. Phys. J. C **77** (2017) 423 [arXiv:1610.06352].
- [31] M. M. Caldarelli, G. Cognola and D. Klemm, *Thermodynamics of Kerr-Newman-AdS black holes and conformal field theories*, Class. Quant. Grav. **17** (2000) 399 [hep-th/9908022].
- [32] D. Kastor, S. Ray and J. Traschen, *Enthalpy and the Mechanics of AdS Black Holes*, Class. Quant. Grav. **26** (2009) 195011 [arXiv:0904.2765].
- [33] M. Cvetič, G. Gibbons, D. Kubiznak and C. Pope, *Black Hole Enthalpy and an Entropy Inequality for the Thermodynamic Volume*, Phys. Rev. D **84** (2011) 024037 [arXiv:1012.2888].
- [34] B. P. Dolan, *Where is the PdV term in the first law of black hole thermodynamics?*, arXiv:1209.1272.
- [35] S. Gunasekaran, R. B. Mann and D. Kubiznak, *Extended phase space thermodynamics for charged and rotating black holes and Born-Infeld vacuum polarization*, JHEP **1211** (2012) 110 [arXiv:1208.6251].